[6]Hager, J. O., Eyi, S., and Lee, K. D., "Multi-Point Design of Transonic Airfoils," Using Optimization," AIAA Aircraft Design Systems Meeting, AIAA Paper 92-4225, Aug. 1992.

Rollup and Near-Field Behavior of a Tip Vortex

D. Birch* and T. Lee†
McGill University, Montreal, Quebec H3A 2K6, Canada
and
F. Mokhtarian‡ and F. Kafyeke§
Bombardier Aerospace, Dorval, Quebec H4S 1Y4, Canada

Introduction

THE vortex system shed from an aircraft wing rolls up rapidly downstream of the aircraft to form two counter-rotating vortices. These vortices may persist for some time after their generation and can induce significant upsetting rolling or pitching motions and thus pose a hazard to other aircraft that penetrate them. Moreover, tip vortices shed from helicopter rotor blades and propellers interact with following blades causing rotor noise and vibration. Therefore, to minimize the wait time of aircraft on the ground and in the air, as well as to reduce the tip-vortex-generated noise and accompanying potential hazards, the tip-vortex-wake characteristics must be measured and predicted accurately and controlled to allow the most efficient use of airport facilities and to ensure flight safety as well.

Numerous experimental, theoretical, and computational investigations have been conducted to improve the understanding of the tip-vortex structure and its dissipation or persistence. However, unlike the usual void of experimental data, a substantial effort has been invested in developing theoretical and numerical models for the rollup process of tip vortices. Excellent reviews of the underlying theories are given by Williams[1] and Spalart.[2] The bulk of the experimental effort has been mainly directed toward finding the rate of change of the tangential velocity and the strength of trailing vortices in the intermediate- or far-field regions, while addressing the issues of vortex development, stability, and breakdown. However, the dynamics of the initial rollup of a tip vortex around the wing tip and its subsequent development in the near field behind the trailing edge have not been studied sufficiently.[3–8] The near-field behavior of a tip vortex is significant in the flow behind canard wings, helicopter blades (a major noise source), sails of submarines, and propeller blades, where control of tip-vortex cavitation to reduce the noise and wear is of extreme importance.

The objective of the present study was to characterize the formation and growth of a tip vortex along the tip of a rectangular high-lift wing and its subsequent development in the near field (up to 1.5 chords downstream of the trailing edge of the wing) by using a miniature seven-hole pressure probe and particle image velocimetry at low Reynolds numbers. Special attention was focused on the effects of airfoil incidence angle, and Reynolds number, and sweep angle on the vortex strength, size, and tangential and axial velocity distributions. It is anticipated that the present measurements will add more information to the understanding of a tip vortex and its prediction.

Experimental Apparatus and Methods

The experiment was carried out in a low-turbulence $0.9 \times 1.2 \times 2.7$ m subsonic wind tunnel. A single-element rectangular high-lift Bombardier Research and Development wing with a chord c of 50.8 cm and a span of 50.8 cm was used to generate the tip vortices. The square-edged airfoil was mounted vertically at the center of the bottom wall of the wind-tunnel test section. The origin of the coordinates was located at the leading edge of the airfoil with x, y, and z aligned with the streamwise, transverse, and spanwise directions, respectively. A miniature seven-hole pressure probe (with an outside diameter of 2.8 mm) was used to measure the three mean velocity components at $x/c = 0.5$–2.5 with the angle of attack $\alpha = 6$ and 10 deg and also at $x/c = 1.5$ with $\alpha = 2$–18 deg. The probe was calibrated *in situ* before the installation of the model. The calibration procedure followed the procedures described by Wenger and Devenport.[9] Eight pressure transducers (seven for the probe and one for tunnel reference total) were used to maximize data rate of the probe measurements system at each measurement location. The pressure signals were sampled at 500 Hz and were recorded on a 586 personal computer through a 16-bit A/D converter board. Probe traversing was achieved through a custom-built computer-controlled traversing system. Data planes taken along the tip and in the near field of the wing model had 49×49 measuring grid points with increments of $\Delta y = \Delta z = 3.2$ mm.

Double-exposure particle image velocimetry (PIV) was also employed in a 50 cm $\times$ 50 cm $\times$ 1.8 m tow tank. Sodium chloride (Fisher S127-3) was added to the water to keep the 70-μm-diam Amberlite fluorescent particles neutrally buoyant. The particles were illuminated with a laser light sheet with a thickness of 1.5 mm and a width of 30 cm. The directional ambiguity was resolved by employing a stepper-motor-driven rotating mirror image shifting technique.[10] The desired particle illuminations and duration were obtained through an electronic shutter (Uniblitz Model LS6T2), triggered by a predetermined time delay signal, in conjunction with a time delay and pulse generator (Hewlett-Packard 8015A). The output of the electronic shutter was also used to actuate the rotating mirror system. The particle images were recorded on Kodak T-Max 3200 black and white film with standard wet processing. The negatives were scanned and digitized by using a Nikon LS-1000 35-mm film scanner and were analyzed by using the AEA Technology VisiFlow PIV postprocessing software to obtain the instantaneous two dimensional velocity and vorticity distributions. Both straight and swept ($\Lambda = 25$ deg) airfoil models, Numerical-Control-machined from aluminum, were tested in the PIV experiment at a chord Reynolds number $Re = 6.7 \times 10^3$.

Results and Discussion

Figure 1 shows the typical mean velocity vectors and vorticity contours of a tip vortex at $x/c = 0.5$–2 and $\alpha = 6$ deg for $Re = 3.25 \times 10^5$. The numerical values shown in the vorticity contours indicate the normalized vorticity levels. The presence of the multiple secondary vortices (indicated by the small patches of vorticity existing between the feeding vortex sheet and the main vortex) at midchord ($x/c = 0.5$) and its wrapping around the main vortex as it progressed down the chord, as well as the subsequent development with distance aft into a progressively stronger tip vortex, can be clearly seen from the vorticity contours. At $x/c = 1.05$, the rollup was complete and a well-defined tip vortex already existed. The results also indicate that at lower Reynolds number, $Re = 1.63 \times 10^5$ (not shown here), the flow structure around the vortex core became considerably less symmetric and that the presence of secondary vortices was much more evident. Further studies with modified tip geometry are needed to quantify the role of the secondary vortices on the tip vortex size and growth.

Received 16 October 2003; revision received 3 January 2003; accepted for publication 4 January 2003. Copyright © 2002 by the American Institute of Aeronautics and Astronautics, Inc. All rights reserved. Copies of this paper may be made for personal or internal use, on condition that the copier pay the $10.00 per-copy fee to the Copyright Clearance Center, Inc., 222 Rosewood Drive, Danvers, MA 01923; include the code 0021-8669/03 $10.00 in correspondence with the CCC.

*Graduate Research Assistant, Department of Mechanical Engineering.
†Associate Professor, Department of Mechanical Engineering. Member AIAA.
‡Section Chief, Advanced Aerodynamics, Department 777. Member AIAA.
§Manager, Advanced Aerodynamics, Department 777. Senior Member AIAA.

Figure 2 shows the variation of the normalized tip-vortex strength Γ/cU at $x/c = 0.5$–2.5 for $\alpha = 6$ and 10 deg with $Re = 1.63$ and 3.25×10^5. The vortex strength was determined from the seven-hole pressure probe velocity measurements. Also shown in Fig. 2 are the PIV results at $Re = 6.7 \times 10^3$. The tip-vortex strength increased with the distance along the tip and reached a maximum value at $x/c = 1.05$, which implies that most of the vorticity was in the concentrated tip vortex immediately downstream of the trailing edge of the wing. At $x/c = 0.9$, the vortex had already reached about 80% of its maximum strength measured at $x/c = 1.05$. Farther downstream of the trailing edge of the airfoil, the overall circulation basically remained constant and was found to be within ±5% variation of the maximum vortex strength. Figure 2 also indicates that, as α increased, the increase in the aerodynamic loadings and the spanwise distribution of circulation on the wing also resulted in an increase in the vortex strength in both the tip region and the near field. The normalized vortex strength, however, was found to decrease with increasing Reynolds number in the present experiment.

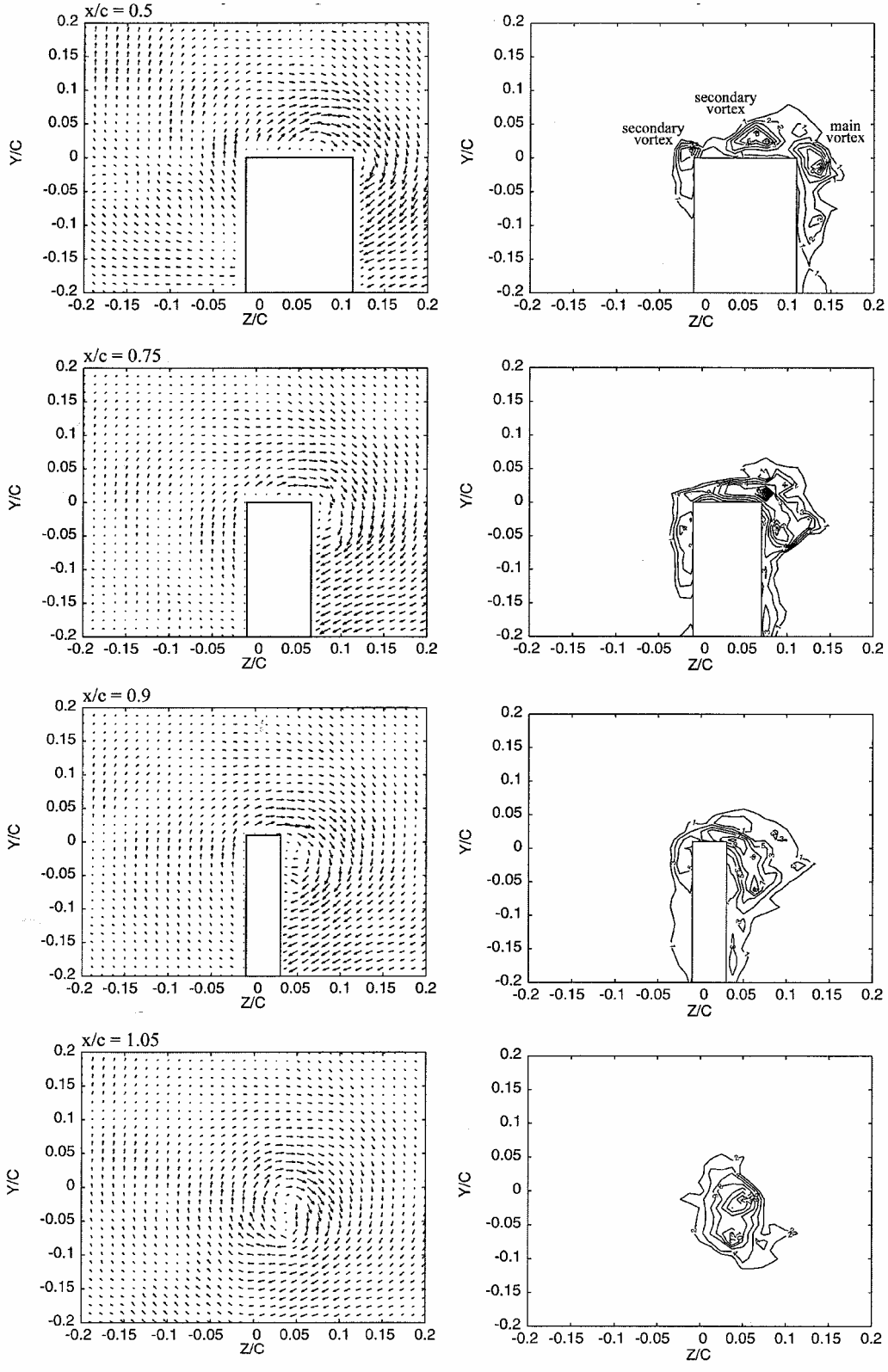

Fig. 1 Typical tip vortex velocity vectors and vorticity contours at various x/c with α = 6 deg.

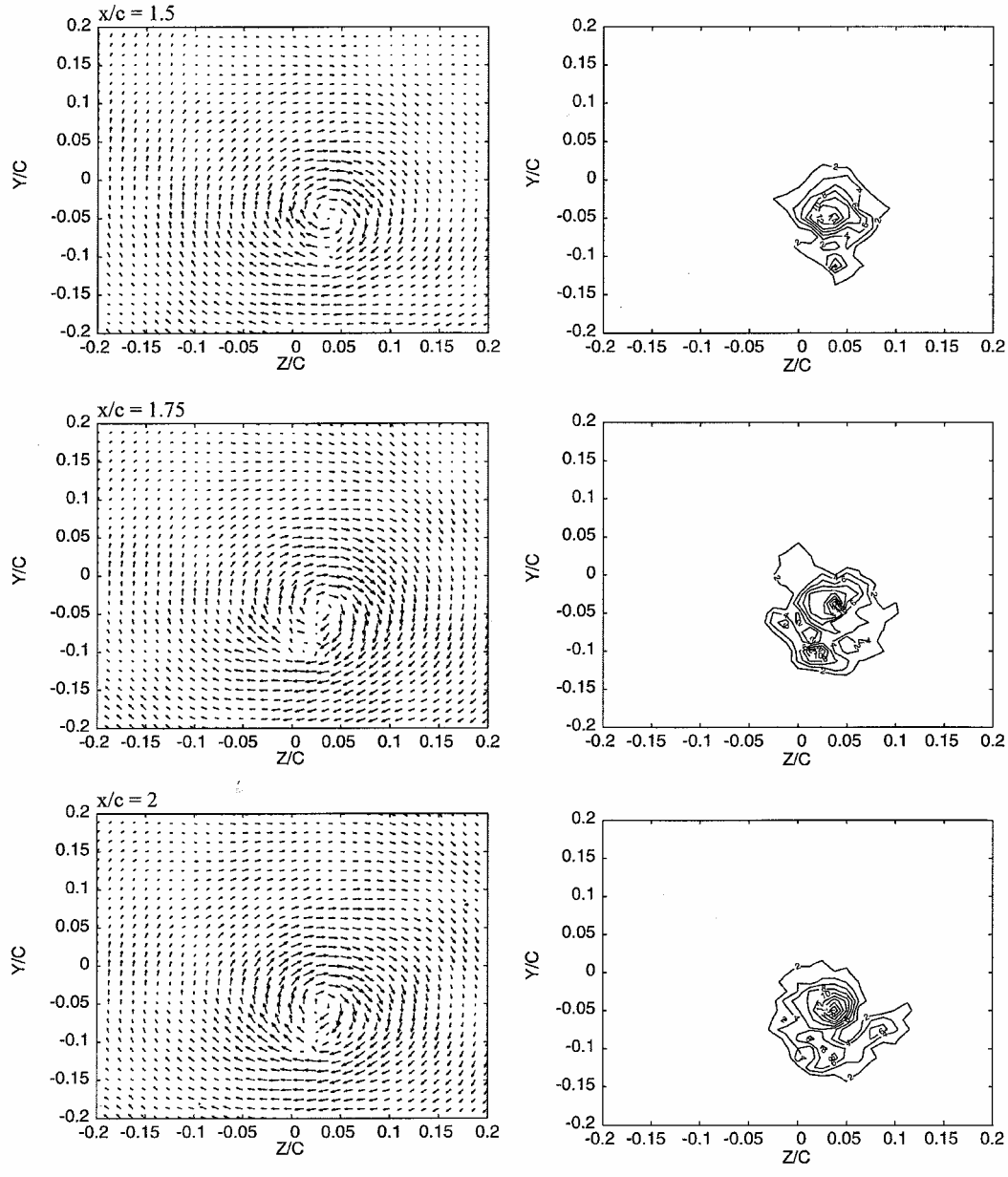

a) Velocity vector map b) vorticity contour

Fig. 1 Typical tip vortex velocity vectors and vorticity contours at various x/c with α = 6 deg (continued).

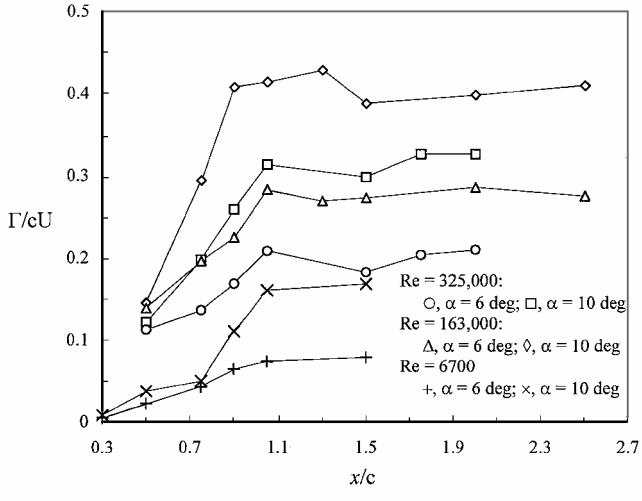

Fig. 2 Variation of normalized tip vortex strength with x/c.

Figure 3 shows the representative effects of α (= 2–16 deg) on the tangential and axial velocity and vorticity distributions across the center of the tip vortex at $x/c = 1.5$ and $Re = 3.25 \times 10^5$. These distributions exhibited all of the qualitative features of the asymptotic viscous/turbulent vortices, such as the zero v_θ at the vortex center, presence of a maximum in the distribution of v_θ within the core (Fig. 3a), the wake- or jetlike core axial flows (Fig. 3b), and the distributed ζ and Γ (Fig. 3c). The variations of the normalized maximum v_θ and core axial velocities and $\zeta_{\max}$, as well as the core radius r_c with α, are summarized in Fig. 4. The magnitudes of these quantities increased with airfoil incidence and reached peak values at $\alpha \approx 12$ and 14 deg for $Re = 1.63$ and 3.25×10^5, respectively. A peak value of $v_{\theta\,\max} = 0.65U$ was observed on the viscous/inviscid boundary layer of the tip vortex for $Re = 1.63 \times 10^5$ (Fig. 4a). Figure 4b shows that, at $\alpha = 2$ deg, the core had developed a large wakelike axial velocity deficit ($\approx 0.75U$). For $\alpha > 6$ deg, the core axial velocity became jetlike. A peak jetlike velocity of $1.72U$ and $1.4U$ was observed at $\alpha = 12$ and 14 deg for $Re = 1.63 \times 10^5$ and 3.25×10^5, respectively. Note that the jet velocity decreased with increasing Reynolds number Re. The core radius, however,

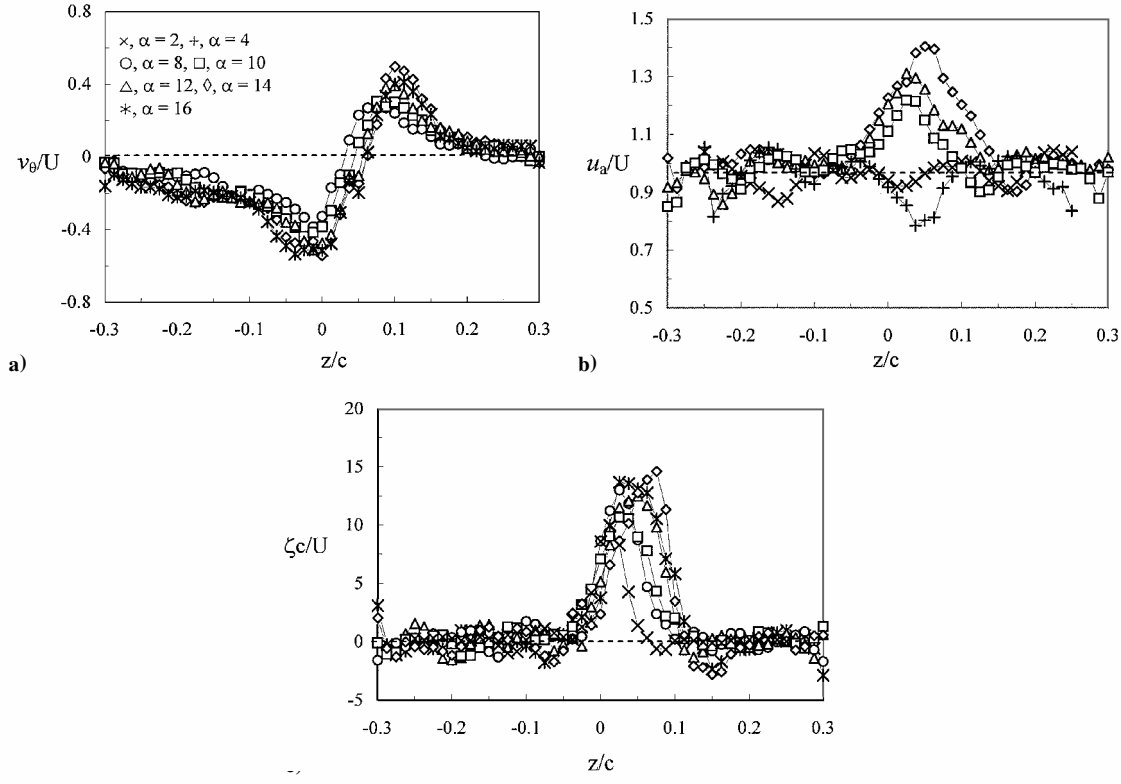

Fig. 3 Typical distributions across the vortex center at x/c = 1.5 and $Re = 3.25 \times 10^5$: a) tangential velocity, b) axial velocity, and c) vorticity.

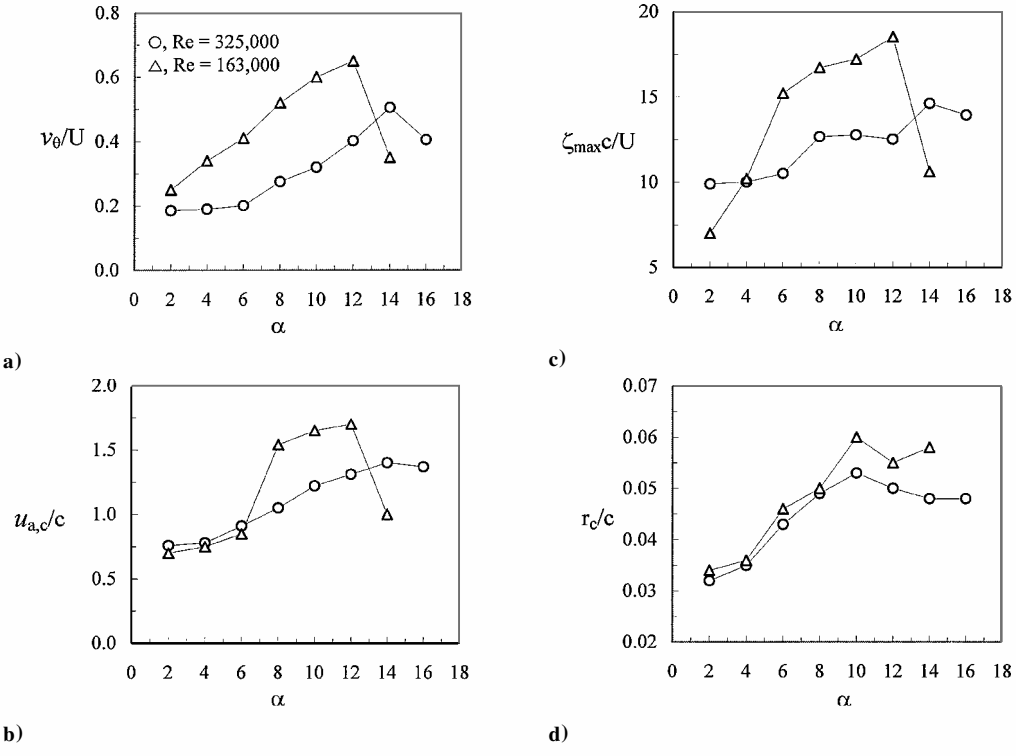

Fig. 4 Variation of a) maximum tangential velocity, core b) axial velocity, and c) vorticity, and d) core radius with α at x/c = 1.5.

was found to be a strong function of α but a weak one of Reynolds number Re (Fig. 4d).

Figure 5 is a summary of the variation of the normalized tip-vortex strength with α at $x/c = 1.5$. The vortex strength was obtained by graphically integrating the areas within contours of constant vorticity. The normalized vortex strength was found to increase with α but decreased with Reynolds number Re. A peak Γ/cU of 0.4013 was observed at $\alpha = 12$ deg for $Re = 1.63 \times 10^5$, an approximately doubled increase in the vortex strength compared to that of $\alpha = 2$ deg. The observed increase in both the strength and size of the tip vortex with increasing α was attributed to the increase in the vorticity shed into the vortex sheet from the boundary layer during its rolling-up into a tip vortex along the tip of the wing model, a phenomenon similar to the boundary-layer tripping and surface roughness effects. The effects of the wing sweep angle ($\Lambda = 25$ deg) on the vortex strength at $Re = 6.7 \times 10^3$ were also examined by using the PIV system. The

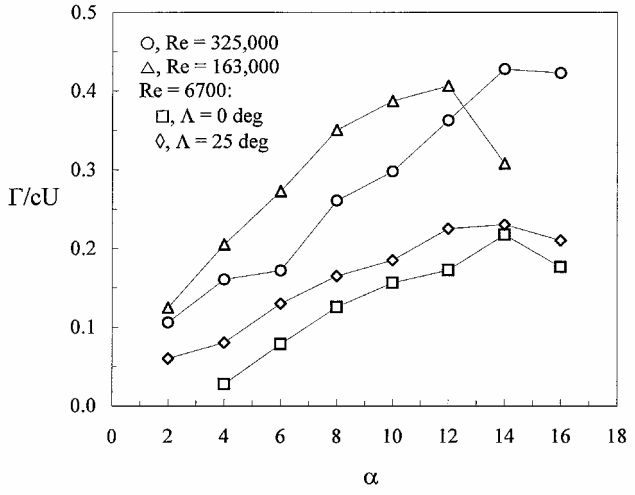

Fig. 5 Variation of normalized tip vortex strength with α at $x/c = 1.5$.

vortex strength was found to increase for a swept wing compared to that of a straight wing.

Conclusions

The formation and growth of a tip vortex in the tip and near-field regions of a single-element rectangular high-lift wing were investigated for $Re \leq 3.25 \times 10^5$. The tip region was dominated by multiple secondary vortex structures. The rollup was almost complete at the trailing edge. The strength of the vortex remained nearly constant up to 1.5 chords downstream of the trailing edge. The core radius and strength and the maximum tangential and core axial velocities of the tip vortex significantly increased with the angle of attack. Also, depending on the angle of attack, the axial velocity in the core could be directed either toward the wing or away from it, that is, of wakelike or jetlike patterns.

Acknowledgments

This work was supported jointly by the Natural Sciences and Engineering Research Council of Canada and Bombardier Aerospace.

References

[1]Williams, G. M., "Viscous Modeling of Wing-Generated Trailing Vortices," *Aeronautical Quarterly*, Vol. 25, May 1964, pp. 143–154.

[2]Spalart, P. R., "Airplane Trailing Vortices," *Annual Review of Fluid Mechanics*, Vol. 30, 1998, pp. 107–138.

[3]Francis, M. S., and Kennedy, D. A., "Formation of a Trailing Vortex," *Journal of Aircraft*, Vol. 16, March 1979, pp. 148–154.

[4]Francis, T. B., and Katz, J., "Observations on the Development of a Tip Vortex on a Rectangular Hydrofoil," *Journal of Fluids Engineering*, Vol. 110, June 1988, pp. 208–215.

[5]Shekarriz, A., Fu, T. C., Katz, J., and Huang, T. T., "Near-Field Behavior of a Tip Vortex," *AIAA Journal*, Vol. 31, No. 1, 1993, pp. 112–118.

[6]Devenport, W. J., Rife, M. C., Liapis, S. I., and Follin, G. J., "The Structure and Development of a Wing-Tip Vortex," *Journal of Fluid Mechanics*, Vol. 312, 1996, pp. 67–106.

[7]Chow, J. S., Zilliac, G. G., and Bradshaw, P., "Mean and Turbulence Measurements in the Near Field of a Wingtip Vortex," *AIAA Journal*, Vol. 35, No. 10, 1997, pp. 1561–1567.

[8]Ramaprian, B. R., and Zheng, Y., "Measurements in Rollup Region of the Tip Vortex from a Rectangular Wing," *AIAA Journal*, Vol. 35, No. 12, 1997, pp. 1837–1843.

[9]Wenger, C. W., and Devenport, W. J., "Seven-Hole Pressure Probe Calibration Utilizing Look-Up Error Tables," *AIAA Journal*, Vol. 37, No. 6, 1999, pp. 675–679.

[10]Zhang, Z., and Eisele, K., "The Two-Dimensional Velocity Caused by the Use of a Rotating Mirror in PIV Flow Field Measurements," *Experiments in Fluids*, Vol. 20, 1995, pp. 106–111.